IEEE Photonics Journal
An IEEE Photonics Society Publication

Open Access

All-Depolarized Interferometric Fiber-Optic Gyroscope Based on Optical Compensation

Volume 6, Number 1, February 2014

Zinan Wang
Yi Yang
Ping Lu
Yongxiao Li
Dayu Zhao
Chao Peng
Zhenrong Zhang
Zhengbin Li

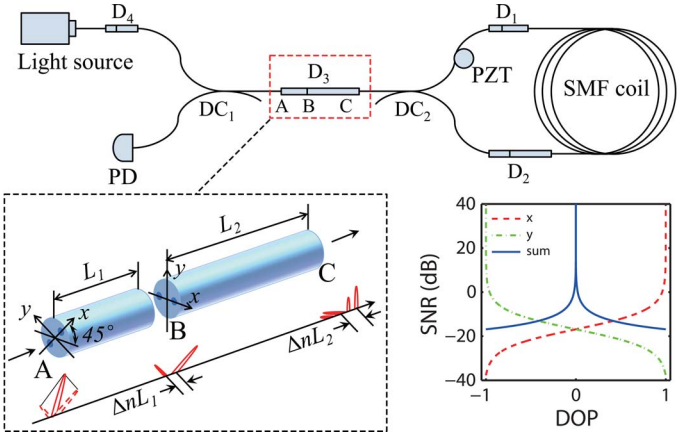

DOI: 10.1109/JPHOT.2014.2299212
1943-0655 © 2014 IEEE

All-Depolarized Interferometric Fiber-Optic Gyroscope Based on Optical Compensation

Zinan Wang,[1] Yi Yang,[1] Ping Lu,[1] Yongxiao Li,[1] Dayu Zhao,[1] Chao Peng,[1] Zhenrong Zhang,[1,2] and Zhengbin Li[1]

[1]State Key Laboratory of Advanced Optical Communication Systems and Networks, Department of Electronics, Peking University, Beijing 100871, China
[2]School of Computer, Electronics and Information, Guangxi University, Nanning 530004, China

DOI: 10.1109/JPHOT.2014.2299212

Manuscript received December 3, 2013; revised December 26, 2013; accepted January 6, 2014. Date of publication January 9, 2014; date of current version January 21, 2014. This work was supported in part by 973 Program of China under Grants 2013CB329205 and 2010CB328203 and in part by the National Natural Science Foundation of China (NSFC) under Grant 61307089. Corresponding author: C. Peng (e-mail: pengchao@pku.edu.cn).

Abstract: We propose and demonstrate a novel configuration for depolarized interferometric fiber-optic gyroscopes (IFOGs). This configuration utilizes optical compensation between two orthogonal polarizations for suppressing errors induced by polarization nonreciprocity. Theoretical analysis shows that it is a new approach different from conventional IFOGs where a polarizer is mandatory. An experimental demonstration of the proposed IFOG (2097-m coil, open-loop configuration) achieves a low bias drift of 0.016°/h in detecting the Earth's rotation rate. Furthermore, this configuration requires no polarizer or any other polarization-maintaining device.

Index Terms: Sensors, fiber-optic gyroscope (FOG), Sagnac effect.

1. Introduction

Interferometric fiber-optic gyroscopes (IFOG) are rotation sensors detecting the phase shift induced by the Sagnac effect [1]. They have been intensively studied for a few decades, and commercial products are available [2]. In IFOGs, the effect of polarization nonreciprocity (PN) is one of the most significant error sources [3]. PN errors would increase the bias drift of detection [4], and hence, degrade the performance of the IFOG.

The conventional approach to suppress PN errors is to maintain the polarization state as much as possible, both in the polarization maintaining IFOG (PM-IFOG) [4]–[8] and the depolarized IFOG [9]–[13]. The basic configuration for these IFOGs is well known as the "minimal scheme", where a polarizer is necessarily used for single polarization reciprocity. Although IFOGs using depolarized light input was also proposed to work in the absence of the polarizer [14], [15], their performance was quite limited due to lack of polarization maintaining. Generally for IFOGs based on the "minimal scheme", PN errors cannot be completely eliminated because of the non-ideality of the polarizer. Therefore, improving the polarization-extinction ratio (PER) is important for conventional IFOGs.

Recently, optical compensation was proposed in the PM-IFOG [16]. PN errors were suppressed in it by utilizing two orthogonal polarizations simultaneously. In this configuration which was referred to as the "dual-polarized IFOG", two orthogonal polarizations of polarization maintaining fiber (PMF) were input incoherently, balanced by a power controller, and then detected independently.

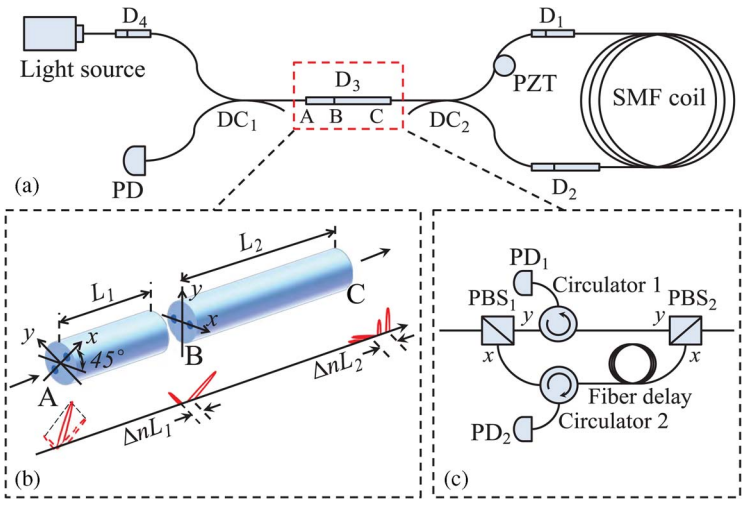

Fig. 1. (a) The all-depolarized IFOG. PD, photodetector; PZT, piezoelectric transducer; D, depolarizers; DC, directional couplers; SMF, single mode fiber. (b) Model for depolarization in the Lyot depolarizer. (c) Replacing D_3 by a depolarizer based on polarization beam splitters (PBS) to observe the compensation phenomenon.

PN errors in two polarizations had opposite polarities, so that we could cancel the errors by adding them up. As a result, PN errors were suppressed. This mechanism of optical compensation reduced the IFOG's bias drift effectively. However, it also increased structural complexity as more polarization selective elements were used.

In this paper, we design and demonstrate a novel depolarized IFOG configuration. Optical compensation is utilized in it to suppress PN errors, with much less complexity than Ref. [16]. An experimental demonstration of it achieves a low bias drift of $0.016^\circ/\mathrm{h}$ in detecting the Earth's rotation rate. While this design has the best ever performance among IFOGs with no polarizer [14], [15], it breaks through the limitation of the "minimal scheme". More importantly, this configuration shows the possibility of low drift IFOGs without any polarizer or any other polarization selective elements.

2. Theory Analysis

Optical compensation requires two incoherent light beams with equal intensity and opposite noise polarities. As shown in Fig. 1(a), we propose a new configuration to realize optical compensation, which we refer to as the "all-depolarized IFOG". Here, two polarizations are input by a Lyot depolarizer D_3 and detected by the same PD.

The Lyot depolarizer made by birefringent fiber (or PMF) is schematically shown in Fig. 1(b). Arbitrarily polarized light entering from Point A will split into two balanced polarizations at Point C. We note L_{dc} as the source's decoherence length, and Δn as the refractive index difference between two axes in PMF. The length $\overline{AB}$ is designed longer than the source's depolarizing length $L_{dp} = L_{dc}/\Delta n$, and $\overline{BC} = 2\overline{AB}$. This ensures that two polarizations are incoherent at Point C. The depolarized light got at Point C is intrinsically equivalent to the dual-polarized light which are capable of optical compensation [16]. Moreover, it has the advantage of dramatically reduced complexity.

The depolarizers D_1 and D_2 inside the coil are for reducing the coherence of PN beams, as the same in conventional depolarized IFOGs [9]–[13]. However, the all-depolarized IFOG requires no polarizer in front of the coil. The depolarizer D_4 is for depolarizing the light source [14], [15]. Most importantly, D_3 is applied to assure the depolarized state at the coil entrance (input port of DC_2).

Theoretical analysis using Jones Matrices is presented in the Appendix section. It proves that PN errors in two polarizations have opposite polarities, so that they can be compensated by simply adding up. The degree of polarization (DOP) at the entrance point of the coil is noted as d. Fig. 2

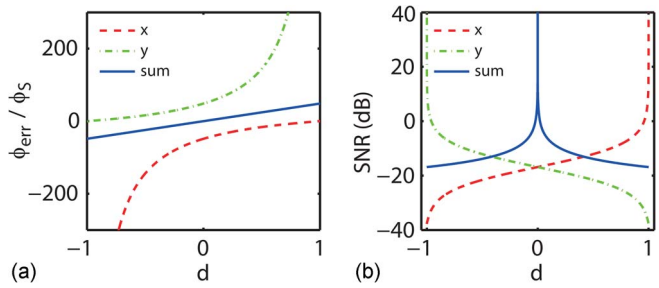

Fig. 2. Performance of two polarizations (red dashed line and green dash-dot line) and the compensated result (blue solid line) evaluated by (a) phase error and (b) signal-to-noise ratio (SNR). d is the degree of polarization.

shows the influence of PN errors in both of the polarizations and also the compensated result. It indicates that the SNR of PN errors is quite high when $d = 0$ (see Appendix for details). It actually reveals an alternative approach for IFOGs to suppress PN errors. Clearly, single polarization operation $(d = \pm 1)$ is one option, which reduces PN errors by elimination PN components. For instance, $d = 1$ means x polarization operation, while y polarization is eliminated by the polarizer. Alternatively, the all-depolarized operation $(d = 0)$ reduces PN errors by compensation. When two polarizations have incoherent light with equal intensity, their noise characteristics result in opposite polarities and will cancel each other. In other words, the result after compensation will have no PN error when $d = 0$.

The matrix analysis reveals two requirements for effective compensation. First, the transition matrices should have the symmetry given by Eq. (3). Secondly, d must be low at the entrance of the coil. In practice, d cannot maintain a low value everywhere in the IFOG, and fortunately this is unnecessary. We verify that only the d value at the entrance of the coil influences the compensation. According to this, a depolarizer must locate just before DC_2, and that is why we apply D_3. In contrast, depolarizing only the source is beneficial but not enough for an optimal design [14], [15]. If D_3 is absent, depolarized light cannot maintain itself while passing through DC_1 and the SMF between two DCs. Particularly, depolarized light will become partially polarized because of the polarization dependent loss (PDL) in DC_1, and light will has an enlarged d at the coil entrance. In conclusion, D_3 is crucial for the IFOG performance, which is also verified by following experiments.

3. Experiments

The experimental setup of the open-loop all-depolarized IFOG is shown in Fig. 1(a). We used an amplified spontaneous emission (ASE) source which had a center frequency at 1550 nm and a band width of 70 nm. Its decoherence length was calculated as $L_{dc} = 34\ \mu$m. The PMF in our depolarizers had $\Delta n = 5 \times 10^{-4}$, thus $\overline{AB}$ in D_4 should be longer than $L_{dp} = L_{dc}/\Delta n = 0.068$ m. Differently in D_1, D_2, and D_3, a much longer depolarizing length L'_{dp} was required because of the possible birefringence in the SMF coil [17]. We used a coil with a 2097 m length and a 0.14 m diameter, and the fiber had a core diameter of 125 μm. For this coil, $L'_{dp} = 1.25$ m is required. All PMF lengths and length differences in these three depolarizes should be larger than L'_{dp}.

For robust performance, we used redundant depolarizing lengths $L_0 = 0.1$ m and $L'_0 = 1.5$ m instead of $L_{dp} = 0.068$ m and $L'_{dp} = 1.25$ m. Accordingly, $\overline{AB}$ parts in $D_1 - D_4$ were chosen 1.5 m, 6 m, 24 m, and 0.1 m, respectively. Every $\overline{BC}$ was twice of its connected $\overline{AB}$. In practical PMF, Δn is unstable because of nonlinear effects and temperature changes, among which temperature influence $d\Delta n/dT \approx 1 \times 10^{-7}$ is dominant. In our design, L_0 and L'_0 was long enough for depolarizing over hundreds of °C. Thus two polarizations were made sure incoherent in our experiments under room temperature range (15–25 °C), and the IFOG avoided temperature related modulations [7].

Theoretically, D_3 is the key component to ensure a low d at the coil entrance. To show its importance, we carried out three experiments with different locations of D_3, while keeping other components unchanged. The experimental conditions were the same, while the detections all

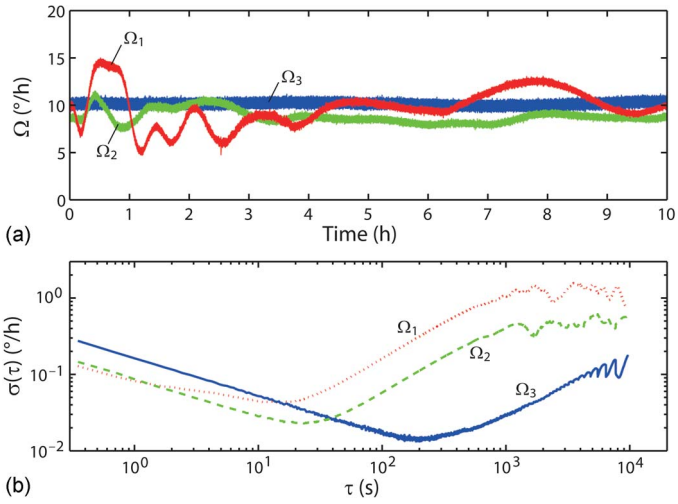

Fig. 3. (a) Long-term output and (b) Allan variance analysis for IFOG structures with different locations of D_3. Ω_1 is for no D_3. Ω_2 is for D_3 located between D_4 and DC_1. Ω_3 is for D_3 between DC_1 and DC_2. Testing conditions and optical components are the same for all the three experimental results.

TABLE 1

Allan variance indices of the all-depolarized IFOG

Quantization noise (rad)	Angle random walk ($°/h^{1/2}$)	Bias drift (°/h)	Rate random walk ($°/h^{3/2}$)	Rate ramp ($°/h^2$)
7.5×10^{-8}	2.8×10^{-3}	1.6×10^{-2}	9.6×10^{-2}	7.7×10^{-2}

targeted the Earth's rotation rate (9.666°/h projected at our laboratory latitude). Detection results were shown in Fig. 3(a), where the sampling rate was 0.35 s and the test length was 10 hours. Ω_1 was measured when D_3 was absent, to verify the necessity of D_3. Ω_2 was measured when D_3 located between D_4 and DC_1, to demonstrate the importance of D_3's location. Ω_3 was for our proposed setup in which D_3 was between DC_1 and DC_2 as shown in Fig. 1(a).

Clearly in Fig. 3(a), Ω_3 was much more stable than either Ω_1 or Ω_2, which verified that putting D_3 between DC_1 and DC_2 was the optimal choice. Without D_3, d was not low enough to ensure effective compensation, and thus Ω_1 had large fluctuations due to PN errors. In the case of Ω_2, although light was well depolarized after D_3, it still had to travel through DC_1 to reach the coil entrance. The well depolarized light became partially polarized due to the inevitable PDL in DC_1, and thus d increased. The comparison between Ω_2 and Ω_3 showed that even with the same total length of depolarizers, placing D_3 right at the coil entrance was especially beneficial for PN error compensation ($d = 5 \times 10^{-3}$ measured) and achieved stable IFOG output.

Allan variance analysis is used to further evaluate the performances [18]. Fig. 3(b) shows the square root of Allan variance $\sigma(\tau)$ versus cluster time τ. Long term drift in Ω_3 is notably reduced, as its curve is much lower than Ω_1 and Ω_2 in the long time scale. The bias drift of Ω_3 is suppressed to 0.016 °/h, indicating a low level of PN errors. Noise performance attributes are given in Table 1. This performance is close to the optically compensated PM-IFOG [16], but with notably reduced complexity.

To verify that the low drift performance was attributed to optical compensation, we designed a test configuration where two polarizations could both be observed. As shown in Fig. 1(c), the test configuration used a PBS based depolarizer instead of the Lyot depolarizer in order to detect two polarizations separately. Afterwards, the summation of two PDs' photocurrents was used as the compensated result. With depolarizing principle equivalent to Fig. 1(b), this structure also generated two polarizations required for compensation. Two polarizations of the input light were split by PBS_1,

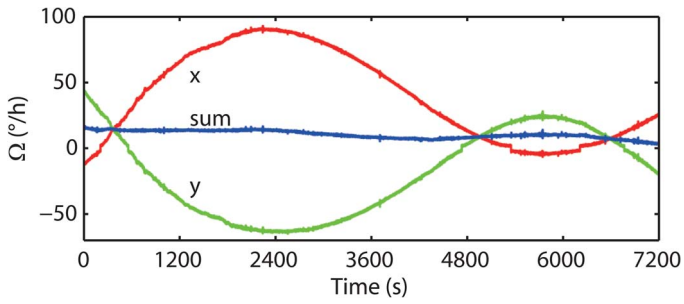

Fig. 4. Experimental observation of optical compensation. The drifts in *x* polarization and *y* polarization are large but with different polarities. In contrast, the drift in the compensated result by summation is notably reduced. There is still drift after compensation because the equivalent configuration did not achieve *d* as low as in the all-depolarized configuration.

and recombined at PBS_2 after a delay difference for decoherence. In our experiment, a 2 m fiber delay was used.

A 2-hour test was carried out on this equivalent configuration under the same experimental condition. Fig. 4 shows the detection results of two polarizations and also the result after compensation. We can see that PN induced drifts in two polarizations are both large but with different polarities, which agrees well with our theoretical prediction in Fig. 2. These large PN errors were caused by unexpected polarization coupling, which varied with temperature. In contrast, the drift in the compensated result was notably reduced. At the combining port of PBS_2, $d = 2 \times 10^{-2}$ was not as low as in the all-depolarized configuration in Fig. 1(a), thus there were still visible drifts after compensation. Nevertheless, this observation verifies that optical compensation is the true reason for PN error reduction in the all-depolarized IFOG.

4. Discussions

All the testing results above verify that the bias drift becomes lower when *d* goes smaller. Comparing with balancing intensity by the power controller in the dual-polarized IFOG [16], lower *d* values can be obtained by the Lyot depolarizer in the all-depolarized IFOG, which is much more effective and less complex.

In PM-IFOGs or conventional depolarized IFOGs, a polarizer with a high PER is indispensable to realize single polarization operation. Differently, the all-depolarized configuration avoids the polarizer. Due to optical compensation, a reduced *d* in the all-depolarized IFOG will have similar performance in suppressing PN noise, compared with an enhanced PER of the polarizer in conventional IFOGs.

Physically, PN errors are caused by various reasons, such as thermal fluctuation and acoustic vibration. Nevertheless, optical compensation only requires that the errors in two polarizations have opposite polarities, which is guaranteed by the intrinsic symmetry of two orthogonal polarizations. Therefore, in the all-depolarized IFOG, PN errors from various noise sources can be suppressed simultaneously. Our experiment under uncontrolled temperature supports this analysis. For further verification, full-range tests are on-going.

Optical compensation is proved effective to further reduce PN errors in the IFOGs without the polarizer [15]. Theoretically, it has equivalent effectiveness for PN error reduction comparing with using polarizers, and thus the all-depolarized IFOG is possible to achieve similar performance as conventional IFOGs with the polarizer. Certainly, non-ideality of Lyot depolarizers degrades the performance of the all-depolarized IFOG, which is similar with non-ideality of conventional polarizers. It requires further efforts to optimize the all-depolarized IFOG to achieve comparative performance of conventional IFOGs, as the conventional ones have been intensively studied for decades. Nevertheless, as no polarizer or any expensive PM components are required, we believe the all-depolarized IFOG is cost-effective. Besides, since Lyot depolarizers are made by fusing PMF which is compliant with fusing other components, no additional fabrication techniques are required. More importantly, the polarizer is proved not mandatory for achieving low drift IFOGs, and an alternative way of using only depolarizers is made available.

5. Conclusion

In conclusion, we have proposed the all-depolarized IFOG configuration by utilizing optical compensation. Theoretical analysis and experimental results show that this configuration is a new approach for suppressing PN errors besides conventional ways. Different from maintaining only a single polarization by a polarizer as in conventional IFOGs, the all-depolarized IFOG configuration achieves low drift through compensating the errors in two polarizations. In this manner, it breaks through the single polarization limitation in the "minimal scheme". In addition, the proposed all-depolarized IFOG requires no PM device and has an all-fiber structure, which makes it convenient for applications.

Appendix
Matrix Analysis

The key parameter in optical compensation is the DOP at the coil entrance. We establish the coordinate system in accordance with the birefringent axes in part $\overline{BC}$. Normalized fields just after Point B can be written as [19]

$$\mathbf{E}_0 = \begin{bmatrix} E_{0x}(t) \\ E_{0y}(t) \end{bmatrix} e^{j\omega_0 t} = \begin{bmatrix} \sqrt{(1+d)/2} \\ \sqrt{(1-d)/2} \end{bmatrix} e^{j\omega_0 t}. \tag{1}$$

Here, $d = (I_{0x} - I_{0y})/(I_{0x} + I_{0y})$ is the DOP at Point B, and ω_0 is the light frequency.

To analyze two polarizations separately, we describe the $\overline{BC}$ part in D_3 by two separate polarizer models with different propagating delay as [14]

$$\mathbf{P}_x = \begin{bmatrix} 1 & 0 \\ 0 & 0 \end{bmatrix} e^{-j\Delta\beta L_{BC}}, \quad \mathbf{P}_y = \begin{bmatrix} 0 & 0 \\ 0 & 1 \end{bmatrix} \tag{2}$$

where $\Delta\beta = \beta_x - \beta_y$ is the propagation constant difference between two birefringent axes of the PMF, and L_{BC} is the length of $\overline{BC}$ in D_3. The delay difference of the two polarizations eliminates the coherence between them. d remains the same through $\overline{BC}$.

In the absence of the Faraday effect, matrices for the Sagnac coil (including DC_2) have reciprocal forms as [3], [14]

$$\mathbf{M}^+ = \begin{bmatrix} C_1 & C_2 \\ C_3 & C_4 \end{bmatrix}, \quad \mathbf{M}^- = \begin{bmatrix} C_1 & C_3 \\ C_2 & C_4 \end{bmatrix}. \tag{3}$$

The superscripts "+" and "−" stands for clockwise (CW) and counterclockwise (CCW), respectively. C_1, C_2, C_3, and C_4 are complex coefficients.

Returned light beams back to point B can be expressed as

$$\mathbf{E}_{ij}^+ = \mathbf{P}_j \mathbf{M}^+ \mathbf{P}_i \mathbf{E}_0 e^{j\phi}, \quad \mathbf{E}_{ij}^- = \mathbf{P}_j \mathbf{M}^- \mathbf{P}_i \mathbf{E}_0 \tag{4}$$

where $\phi = \phi_S + \Delta\phi(t)$, includes both the Sagnac phase ϕ_S and the modulation phase $\Delta\phi(t)$. The subscripts $i, j \in \{x, y\}$, describe the coupling from polarization i to j. Hence, the intensity in the x and y polarizations are obtained as

$$\begin{aligned} I_x &= \left\langle \left| \mathbf{E}_{xx}^+ + \mathbf{E}_{xx}^- + \mathbf{E}_{yx}^+ + \mathbf{E}_{yx}^- \right|^2 \right\rangle \\ &= I_{x0} + q_x \cos\phi + p_x \sin\phi \\ &= I_{x0} + \sqrt{p_x^2 + q_x^2} \cos(\phi - \phi_{err}^x) \end{aligned} \tag{5}$$

$$\begin{aligned} I_y &= \left\langle \left| \mathbf{E}_{yy}^+ + \mathbf{E}_{yy}^- + \mathbf{E}_{xy}^+ + \mathbf{E}_{xy}^- \right|^2 \right\rangle \\ &= I_{y0} + q_y \cos\phi + p_y \sin\phi \\ &= I_{y0} + \sqrt{p_y^2 + q_y^2} \cos(\phi - \phi_{err}^y) \end{aligned} \tag{6}$$

where I_{x0} and I_{y0} are direct-current components, ϕ_{err}^{x} and ϕ_{err}^{y} are PN induced phase errors in two polarizations, respectively. The phase errors are derived as

$$\begin{aligned}
\phi_{err}^{x} &= \arctan(p_x/q_x) \\
\phi_{err}^{y} &= \arctan(p_y/q_y) \\
p_x &= -(1-d)|C_2C_3|\Gamma(z_{23})\sin\phi_{23} \\
q_x &= |C_1|^2(1+d)+(1-d)|C_2C_3|\Gamma(z_{23})\cos\phi_{23} \\
p_y &= (1+d)|C_2C_3|\Gamma(z_{23})\sin\phi_{23} \\
q_y &= |C_4|^2(1-d)+(1+d)|C_2C_3|\Gamma(z_{23})\cos\phi_{23}.
\end{aligned} \tag{7}$$

Here, $\Gamma(z)$ is the source's degree of coherence [13], z_{23} is the birefringent delay induced by $C_2C_3^*$, and ϕ_{23} is the phase of $C_2C_3^*$.

p_x and p_y have different signs, showing that the phase errors in two polarizations have opposite polarities. Without coherence between the two polarizations, light intensity is directly added up at the PD as

$$\begin{aligned}
I_{sum} &= I_{x0}+I_{y0}+(q_x+q_y)\cos\phi+(p_x+p_y)\sin\phi \\
&= I_{DC}+k_{sum}\cos\left(\phi-\phi_{err}^{sum}\right)
\end{aligned} \tag{8}$$

where k_{sum} is the contrast coefficient, and ϕ_{err}^{sum} is the phase error after compensation. They are given by

$$k_{sum} = \sqrt{(p_x+p_y)^2+(q_x+q_y)^2} \tag{9}$$

$$\begin{aligned}
\phi_{err}^{sum} &= \arctan\frac{p_x+p_y}{q_x+q_y} \\
&= \arctan\frac{2d|C_2C_3|\Gamma(z_{23})\sin\phi_{23}}{|C_1|^2(1+d)+|C_4|^2(1-d)+2|C_2C_3|\Gamma(z_{23})\cos\phi_{23}}.
\end{aligned} \tag{10}$$

The final phase error ϕ_{err}^{sum} decreases with the absolute value of d, and $\phi_{err}^{sum}=0$ when $d=0$.

References

[1] E. J. Post, "Sagnac effect," *Rev. Mod. Phys.*, vol. 39, no. 2, pp. 475–493, Apr. 1967.
[2] H. C. Lefèvre, *The Fiber-Optic Gyroscope*. Norwood, MA, USA: Artech House, 1993.
[3] I. A. Andronova and G. B. Malykin, "Physical problems of fiber gyroscopy based on the Sagnac effect," *Phys. Usp.*, vol. 45, no. 8, pp. 793–817, Aug. 2002.
[4] S. L. A. Carrara, B. Y. Kim, and H. J. Shaw, "Bias drift reduction in polarization-maintaining fiber gyroscope," *Opt. Lett.*, vol. 12, no. 3, pp. 214–216, Mar. 1987.
[5] R. Ulrich and M. Johnson, "Fiber-ring interferometer-polarization analysis," *Opt. Lett.*, vol. 4, no. 5, pp. 152–154, May 1979.
[6] R. Ulrich, "Fiber-optic rotation sensing with low drift," *Opt. Lett.*, vol. 5, no. 5, pp. 173–175, May 1980.
[7] D. Kim and J. Kang, "Sagnac loop interferometer based on polarization maintaining photonic crystal fiber with reduced temperature sensitivity," *Opt. Exp.*, vol. 12, no. 19, pp. 4490–4495, Sep. 20, 2004.
[8] Z. Wang, Y. Yang, Y. Li, X. Yu, Z. Zhang, and Z. Li, "Quadrature demodulation with synchronous difference for interferometric fiber-optic gyroscopes," *Opt. Exp.*, vol. 20, no. 23, pp. 25 421–25 431, Nov. 5, 2012.
[9] K. Böhm, P. Marten, K. Petermann, E. Weidel, and R. Ulrich, "Low-drift fiber gyro using a superluminescent diode," *Electron. Lett.*, vol. 17, no. 10, pp. 352–353, May 14, 1981.
[10] R. J. Fredricks and R. Ulrich, "Phase error-bounds of fiber gyro with imperfect polarizer depolarizer," *Electron. Lett.*, vol. 20, no. 8, pp. 330–332, Apr. 12, 1984.
[11] E. Jones and J. W. Parker, "Bias reduction by polarisation dispersion in the fibre-optic gyroscope," *Electron. Lett.*, vol. 22, no. 1, pp. 54–56, Jan. 2, 1986.
[12] B. Szafraniec and J. Blake, "Polarization modulation errors in all-fiber depolarized gyroscopes," *J. Lightw. Technol.*, vol. 12, no. 9, pp. 1679–1684, Sep. 1994.
[13] B. Szafraniec and G. A. Sanders, "Theory of polarization evolution in interferometric fiber-optic depolarized gyros," *J. Lightw. Technol.*, vol. 17, no. 4, pp. 579–590, Apr. 1999.
[14] G. A. Pavlath and H. J. Shaw, "Birefringence and polarization effects in fiber gyroscopes," *Appl. Opt.*, vol. 21, no. 10, pp. 1752–1757, May. 15, 1982.

[15] W. K. Burns and A. D. Kersey, "Fiber-optic gyroscopes with depolarized light," *J. Lightw. Technol.*, vol. 10, no. 7, pp. 992–999, Jul. 1992.
[16] Y. Yang, Z. Wang, and Z. Li, "Optically compensated dual-polarization interferometric fiber-optic gyroscope," *Opt. Lett.*, vol. 37, no. 14, pp. 2841–2843, Jul. 15, 2012.
[17] R. Ulrich, S. C. Rashleigh, and W. Eickhoff, "Bending-induced birefringence in single-mode fibers," *Opt. Lett.*, vol. 5, no. 6, pp. 273–275, Jun. 1980.
[18] *IEEE Standard Specification Format Guide and Test Procedure for Single-Axis Interferometric Fiber Optic Gyros*, IEEE Std. 952-1997 (2008R), 1997.
[19] R. F. Mathis, B. A. May, and T. A. Lasko, "Polarization coupling in unpolarized interferometric fiber optic gyros (IFOGs): Effect of imperfect components," in *Proc. SPIE*, 1994, vol. 2292, pp. 283–291.